

Advances in the Parameter Space Concept for Picometer Precise Crystal Structure Refinement – A Resolution Study

MATTHIAS ZSCHORNAK,^{a,b*} CHRISTIAN WAGNER,^a MELANIE NENTWICH^c AND
KARL F. FISCHER^d

^a*Center for Efficient High Temperature Processes and Materials Conversion ZeHS,
TU Bergakademie Freiberg, Winklerstr. 5, D-09596 Freiberg, Germany,* ^b*Institute of
Experimental Physics, TU Bergakademie Freiberg, Leipziger Str. 23, D-09596
Freiberg, Germany,* ^c*Deutsches Elektronen-Synchrotron DESY, Notkestr. 85,
D-22607 Hamburg, Germany,* and ^d*Institute of Experimental Physics, Universität des
Saarlandes, D-66123 Saarbrücken, Germany.*
E-mail: matthias.zschornak@physik.tu-freiberg.de

Parameter Space Concept; high resolution; high quality; validation and reproducibility in structural science;

X-ray diffraction; resonant contrast; pm resolution; pseudo-symmetry

Abstract

The *Parameter Space Concept* (PSC) is an alternative approach to solve and refine (partial) crystal structures from very few pre-chosen X-ray or neutron diffraction amplitudes without the use of Fourier transforms. PSC interprets those amplitudes as piecewise analytic hyper-surfaces, so-called isosurfaces, in the Parameter Space, which is spanned by the spatial coordinates of all atoms of interest. The intersections of all isosurfaces constitute the (possibly degenerate) structure solution.

The present feasibility study investigates the La and Sr split position of the potential high-temperature super-conductor $(\text{La}_{0.5}\text{Sr}_{1.5})\text{MnO}_4$, $I4/mmm$, with a postulated total displacement between La and Sr of a few pm by theoretical amplitudes of pre-selected $00l$ reflections ($l = 2, 4, \dots, 20$). The revision of 15 year old results with modern computing equipment enhances the former simplified model by varying the scattering power ratio $f_{\text{La}}/f_{\text{Sr}}$ (as exploitable by means of resonant scattering contrast at synchrotron facilities) and revealed one of the two originally proposed solutions irrevocably as a “blurred” pseudo-solution.

Finally, studying the resolution limits of PSC as a function of intensity errors by means of Monte-Carlo simulations shows that both, the split can only be resolved for sufficiently low errors and a theoretical resolution down to ± 0.19 pm can be achieved for this specific structural problem.

1. Introduction

Within the last 15 years, the *Parameter Space Concept* (PSC) was theoretically developed by Fischer, Kirfel and Zimmermann [1–6] as alternative approach to solve and refine (partial) crystal structures from diffraction amplitudes without the use of Fourier transforms. The latter map the electron or scattering density distribution $\rho(x, y, z)$ for $0 \leq x, y, z < 1$ in the crystallographic unit cell (or in its asymmetric part). In contrast, PSC is based on the dependence of scattering amplitudes on the exact values of the structural parameters and their correlations. Hereby, the intrinsically as free considered $3m$ parameters of an m atomic structure span its $3m$ -dimensional *Parameter Space* (PS). As in the framework of structure factors F , each combination of coordinates results in a specific amplitude $|F(hkl)|$ for a reflection hkl . If the experimental amplitude of a reflection is known from measurements, the possible coordinate combinations ensuring this amplitude are restricted by a piecewise analytic hyper-surface,

a manifold of $(3m - 1)$ dimensions called *isosurface* of $|F(hkl)|$. Generally, each two intersecting isosurfaces will reduce the possible structure solutions by one dimension. The solution vector is the intersection of all such isosurfaces [5].

An essential feature of PSC is: If more than one solution reproduces the experimental observations within the accuracy limit, the PSC presents all those solutions, in contrast to conventional methods. Furthermore, the PSC offers in principle a much higher spatial resolution than that of a conventional scattering density distribution $\rho(x, y, z)$ obtained by Fourier transformation. The “optical” resolution of Fourier methods is limited by the maximum momentum transfer $|\vec{Q}|$ (thus proportional to the largest reciprocal lattice vector) of a “full” spherical data set, if all its structure factors $F(hkl)$ are assumed error-free and correctly phased. In contrast, the resolution of PSC results is not *a priori* limited by this threshold, provided the number $3m$ of parameters is smaller than or equal to the number of applied independent amplitudes.

To keep computing demand under control, we simplify the problem by 1-dimensional projections of the structure onto the x , y , and z axes and subsequently interconnecting those projected solutions [7]. For a 1-dimensional structure projection, *e. g.* onto the z axis, only m independent isosurfaces for $|F(l)| := |F(00l)|$ are needed to define the “solution point” for the structure projection onto this axis.

2. The Object and its PSC-Handling

The structure of $(\text{La}_{0.5}\text{Sr}_{1.5})\text{MnO}_4$ has space group $I4/mmm(139)$, with lattice parameters $a = 3.863 \text{ \AA}$, $c = 12.421 \text{ \AA}$ [8]. In the reported structure La and Sr occupy the same equal point $(0, 0, z_0)$ with an originally determined $z_0 = 0.35816_3$ (thus, also $0.5 - z_0 = 0.14184$). At the same time, multipole refinements on accurate high-energy data (100 keV, *i. e.* $\lambda = 0.124 \text{ \AA}$) up to $\sin \theta / \lambda = 1.1 \text{ \AA}^{-1}$ and $R(F) = 0.009$ were performed [9] with a resolution of about 1 pm. These data indicated the possibility of split

positions for the cations La and Sr with a difference in z of $\Delta z := |z_{\text{Sr}} - z_{\text{La}}| \approx 0.0016$, *i. e.* ≈ 2.0 pm, well beyond the limit of resolution for this data set. To have a reliable estimate from *ab-initio* electronic structure calculations we performed preliminary modeling by means of density functional theory (DFT)¹ in a $2 \times 2 \times 1$ supercell. The results indicate a split of about $\Delta z = 0.034$ (≈ 4.2 pm).

Instead of doing, *e. g.*, a least-squares refinement on all structure parameters based on a full 3-dimensional data set, this problem can be investigated with PSC, as has already been done by Kirfel *et al.* [11]. Since the free coordinates only point along the c direction, the problem can be treated in a 1-dimensional primitive lattice with period of $c' = c/2$ by employing only $00l$ reflections, which account for the projection of the structure onto $[001]$ [11]. Considering La/Sr partial structure contributions according to the *Equal Point Atom* (EPA) model upon using the simplification $f_{\text{La}} = f_{\text{Sr}} = 1$, the corresponding PSC model for the La/Sr split position is a centric 2-dimensional Parameter Space \mathcal{P}^2 . The permutation symmetry is reflected in the small asymmetric unit of the *Partial Geometric Structure Factor* G_2 within the Parameter Space $\mathcal{P}^2 = z_{\text{La}} \otimes z_{\text{Sr}}$, as indicated with the grey shaded area in Fig. 1 (*cf.* Fig. 1 in [11]). Here, G_2 is defined as $G_2(l) = s(l)g(l) = 2 \sum_{j=\text{Sr,La}} \cos 2\pi l z_j$, where $s(l)$ depicts the sign and $g(l)$ the amplitude of the expression. In general, the *Geometric Structure Factor* $G(l) = \sum_{j=1}^m \cos 2\pi l z_j$ represents the full centrosymmetric structure of m atoms in the EPA model, whereas $F(l)$ denotes the conventional structure factor.

The computed $F(l)$ values comply with the demands of the “Karle separation” [12] leading to dispersion-free partial structure amplitudes of the cations in question. The so-called *Unitary Structure Amplitudes* $U(l) = |F(l)| / \sum_j f_j(l) \leq 1$ transform into geometric structure amplitudes $g(l)$ by $m \cdot U(l) = g(l) = |\sum_j \cos 2\pi l z_j|$, as done by [2, 11].

¹ VASP code [10] with generalized-gradient approximation using the Perdew-Burke-Ernzerhof functional ($\Delta k < 0.02 \times 2\pi \text{ \AA}^{-1}$, 600 eV plane-wave cutoff)

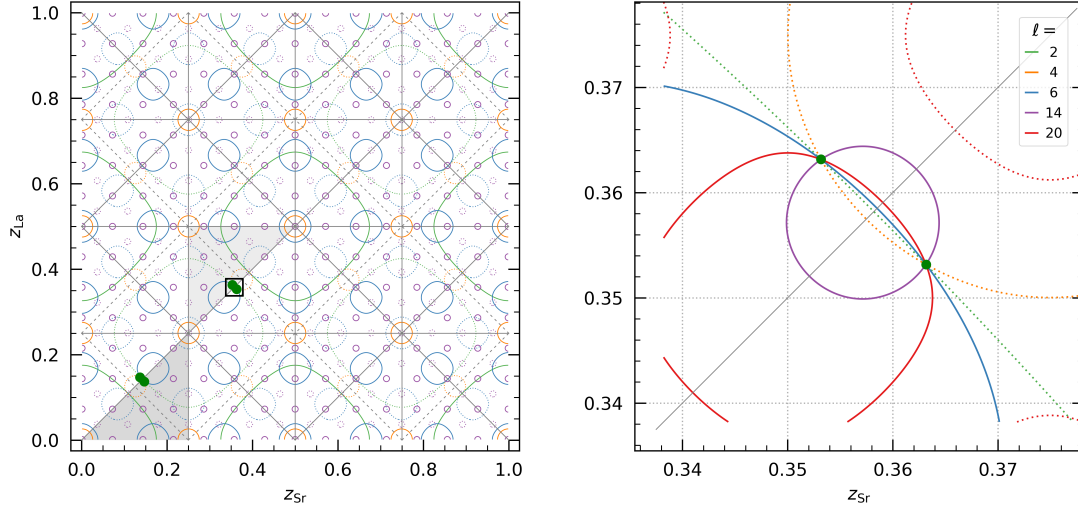


Fig. 1. The 2-dimensional Parameter Space $z_{\text{La}} \otimes z_{\text{Sr}}$ for the La/Sr Partial Geometric Structure Factors $G_2(l)$ of $(\text{La}_{0.5}\text{Sr}_{1.5})\text{MnO}_4$, $I4/mmm$. The data are visualised in the full functional region (left) and the magnified region of interest (right) as isosurfaces, including positive (solid lines) and negative signs (dotted lines). The permutation symmetry of \mathcal{P}^2 adds an exact pseudo-solution $z_{\text{La}}^* = 0.35316$, $z_{\text{Sr}}^* = 0.36316$ to the presumed split position $z_{\text{La}} = 0.36316$, $z_{\text{Sr}} = 0.35316$ (green dots). The grey shaded areas depict two different, but equivalent asymmetric units: the conventional one (dark grey) and the one used in literature (light grey), for better comparison. Grey solid lines depict mirrors and grey dashed lines anti-mirrors.

In the early test calculations, Kirfel *et al.* assumed a rather large split of $\Delta z = 0.01$ [11], as they did not expect to reach the (much smaller) estimation of the experiment [9]. The PSC approach then recovered the positions $z_{\text{La}} = 0.349$, $z_{\text{Sr}} = 0.362$ with a split of $\Delta z = 0.01_3$. Alternatively, they also had determined the z coordinates by a batch of 300 calculations as $z_{\text{Sr}} - z_{\text{La}} = 0.014_2 \dots 0.015_0$ with estimated errors between $0.002_1 \dots 0.003_8$ (from Gaussian distribution fits and their single half-widths). For this approach, they put a maximum relative statistical data error of 10 % or 20 %, respectively, onto the G_2 values [2]. Both results reflect the identified split position close to the presumed $z_{\text{Sr}} - z_{\text{La}} = 0.360 - 0.350 = 0.010$, nevertheless with a significant offset of about 30 %.

As a basis for the subsequent analysis of smaller and more reasonable splits, we recre-

ated these calculations within the EPA model with modern computing equipment, only using the Sr/La substructure with the originally applied split of $\Delta z = 0.01$ for comparison and fixing the MnO substructure. We calculated the diffraction amplitudes from the $(\text{La}_{0.5}\text{Sr}_{1.5})\text{MnO}_4$ structure as determined by Senff *et al.* at room temperature [8]. Figure 1 shows the corresponding isolines for the reflections $00l$ with $l = 2, 4, \dots, 20$ for this very simple case. The PSC approach finds the exact solution without offset. Due to the permutation symmetry of \mathcal{P}^2 , a second exact pseudo-solution is evident with interchanged La/Sr z -coordinates. None of the five selected reflections used in this figure had small amplitudes (also complies to Fig 2); they were chosen because their isolines intersect at large angles, while others present severe correlation effects and hence do not provide optimal resolution results.

3. Resolution Studies

The following resolution study improves the performance of the simple PSC approach used by Kirfel *et al.* pushing the PSC method to its limits in dependence on different data qualities for this specific structural case. This goal is achieved on the one hand by abandoning the EPA model and taking into account a series of smaller splits, and on the other hand by introducing enhanced (resonant) scattering contrast. The $00l$ reflection intensities were calculated for $l = 2, 4, \dots, 20$ at a wavelength of $\lambda = 0.7705 \text{ \AA}$ (*i. e.* 15 keV) and, in addition, at $\lambda_e = 0.7697 \text{ \AA}$ (*i. e.* 16.1 keV), which is just below the excitation of the Sr- K absorption edge. These complementary calculations vary the scattering strength specifically of Sr and artificially enhance the contrast by means of dispersion-free and dispersion-modified $|F(l)|$ based on a negative f'_{Sr} (while $f''_{\text{Sr}} \approx 0$ [13]), since the structural scenario is not altered. This resonant contrast has been widely used in Resonant X-ray Diffraction for accurate crystal structure refinements (*e. g.* [14–16]).

In short, the following consecutive enhancements cover: (a) different real f (thus breaking the permutation symmetry of the EPA model, see solutions in Fig. 1), (b) some smaller Δz model assumptions and respective PSC resolution for several data qualities, as well as (c) resolution enhancement by energy dispersive amplitude differences and respective resonant contrast.

Step 1: Going beyond the Equal Point Atom Model

In a first step, the scattering contribution of La and Sr was treated with the conventional scattering factors $f_{\text{Sr}} \neq f_{\text{La}}$ (with $f''_{\text{Sr}} \approx 0$). While irrelevant for the EPA solution, now a qualitative choice has to be made regarding the displacement direction of La and Sr. Following our preliminary DFT results, we define La with the larger z coordinate. This induces a break of permutation symmetry in the data, doubling the 2-dimensional asymmetric unit (Fig. 2, in comparison to Fig. 1), as expected. The disproportionated La/Sr scattering strength results in elongation and contraction of the isosurfaces, which lifts the mirror along $z_{\text{Sr}} = z_{\text{La}}$. Additional qualitative changes of the isosurfaces' landscapes originate from the inclusion of the MnO_4 partial structure. By fixing the known MnO_4 contribution, the here defined “core question” of determining two z parameters can be approached independently of the noise from all the other structural parameters (and from almost all 3-dimensional experimental measurements). Again, the PSC approach finds the exact solution without offset. Now, the exact pseudo-solution $(z_{\text{Sr}}^*, z_{\text{La}}^*)$ formerly at inverted coordinates (*cf.* with Fig. 1) shifts to the coordinates $z_{\text{Sr}}^* \approx 0.3605$, $z_{\text{La}}^* \approx 0.3499$.

For the discussed Sr/La split position, the “broken symmetry” may result either in two statistically occupied, equivalent 4e positions $(0, 0, z)$ for Sr and La, keeping the space group $I4/mmm$, or in an asymmetric split of the position, the reduction of the space group symmetry and possibly a superstructure of multiple cell volume. This

cannot be answered at present without experimental details.

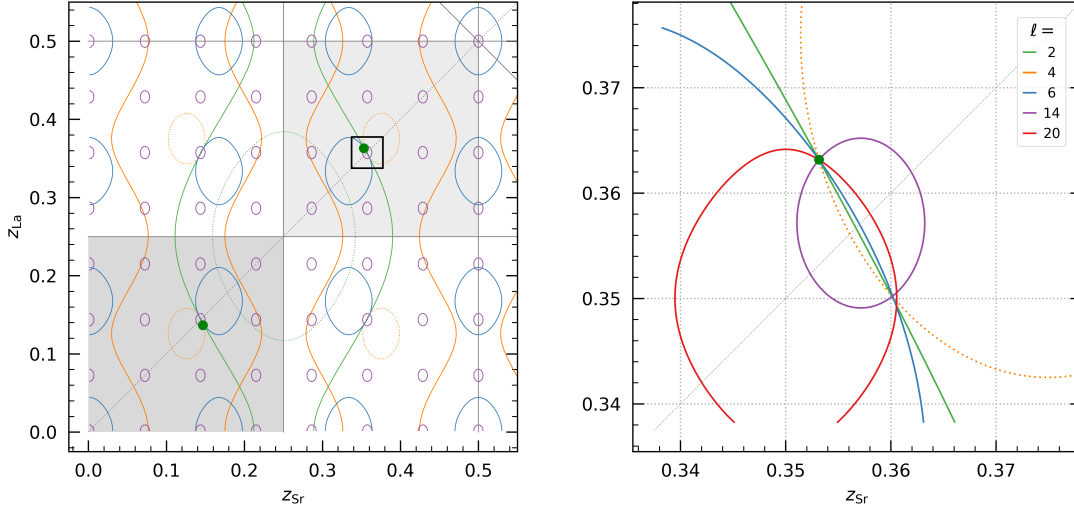


Fig. 2. The 2-dimensional Parameter Space $z_{\text{Sr}} \otimes z_{\text{La}}$ for the complete structure of $(\text{La}_{0.5}\text{Sr}_{1.5})\text{MnO}_4$, $I4/mmm$, with computed diffraction data $F(l)$ in the first quadrant (left) and the magnified region of interest (right). The functions are visualised as isosurfaces including positive (solid lines) and negative signs (dotted lines), with asymmetric units and mirrors in analogy to Fig. 1. The mirror along $z_{\text{Sr}} = z_{\text{La}}$ lifts by loss of permutation symmetry from $f_{\text{Sr}} \neq f_{\text{La}}$ and the pseudo-solution $(z_{\text{La}}^*, z_{\text{Sr}}^*)$ with approximately interchanged coordinates shifts.

Figure 2 reveals that in general isosurfaces (here isolines) of larger l have stronger curvatures and higher gradients due to shorter periodicities, which is valid for the Parameter Space of any dimension. In terms of contrast, gradients may become especially high for isosurfaces of small or vanishing amplitudes (though varying along the isosurfaces). This can be seen from the development of the structure factor close to zero intensity for small atomic displacements \vec{u}

$$\begin{aligned}
 F(E, \vec{Q}) &= \sum_{j=1}^m o_j f_j(E, \vec{Q}) e^{-M_j} e^{i\vec{Q}\vec{r}_j} \\
 &= \underbrace{F|_{\vec{u}=0}}_{\rightarrow 0} + \left. \frac{\partial F}{\partial u^k} \right|_{\vec{u}=0} \langle u^k \rangle + \frac{1}{2} \left. \frac{\partial^2 F}{\partial u^k \partial u^l} \right|_{\vec{u}=0} \langle u^k u^l \rangle + \dots \\
 &\approx o_j f_j e^{-M_j} e^{i\vec{Q}\vec{r}_j^0} \cdot \left(iQ_k \langle u^k \rangle - \frac{1}{2} Q_k Q_l \langle u^k u^l \rangle \right),
 \end{aligned} \tag{1}$$

with occupancy of the crystallographic site o_j and the Debye-Waller factor e^{-M_j} taking into account the reduction of the scattering amplitude due to the uncertainty in the position \vec{r}_j of atom j . Thus, these regions of high contrast provide the largest change of the amplitude's interference balance, accompanied with enhanced sensitivity reflecting not only the correlated structural dependencies respecting the direction of the gradient, but generally of any individual atomic position as well. Only for very specific correlated parameter changes along the $m - 1$ dimensional manifold of the isosurface, the balance of destructive interference can be kept fulfilled. This enhanced sensitivity for positional changes is similar to the high contrast for atomic displacements achieved by the Resonantly Suppressed Diffraction method, which varies the scattering power of certain atomic species by means of dispersion corrections [16].

Error-free isosurfaces of a given amplitude have no thickness along their gradient vectors, and are thus manifolds of no volume in the respective Parameter Space. Yet, a certain thickness occurs as soon as data sets have an error distribution. However, this non-vanishing volume for the solution space is less pronounced along large gradients. Thus, for obtaining a high resolution, the optimal reflections can be selected from a given set of observations (provided the parameter region investigated is sufficiently close to the final result) choosing high order, low amplitude, minimal $|F|/|l|$, and low correlation with other isosurfaces (*i. e.* large intersection angles). If those (few) optimal reflections are measured more accurately, they provide the best basis for high resolution at low cost for synchrotron or neutron beamtimes. To select a set of low-correlated reflections, possible candidates are easily identifiable in the Parameter Space from isosurface representations as well: high correlation coefficients between two parameters show themselves on the basis of nearly parallel isosurfaces, *i. e.* by small intersection angles. Optimal parameters are thus obtained by selecting reflection amplitudes that intersect orthogonal at best.

Step 2: Variations of Atomic Scattering Power

To assess the general impact of resonant scattering contrast onto the positional resolution, *e.g.* specifically in the smooth pre-edge regions of La and Sr without fine structure oscillations due to absorption effects, we varied the scattering strength ratio $f_{\text{La}}/f_{\text{Sr}}$, while keeping the product $f_{\text{La}} \cdot f_{\text{Sr}}$ fixed. Within the chosen range of $f_{\text{La}}/f_{\text{Sr}}$ up to a scaling factor of 10, the coordinates of the sharp solution vector have to remain constant, of course, as they resemble the true structural positions. However, the position of the pseudo-solution changes significantly in the relative coordinates (Fig. 3 (a)). As is evident, this qualitative displacement of the pseudo-solution vector in Parameter Space scales with the variation of the scattering power. This conclusion will generally hold for any structural pseudo-symmetry scenario with a false solution close to the true one. Since the element specific weights of the partial structure contributions are directly varied, the isosurfaces' boundary conditions of fixed amplitudes (Fig. 3 (b,c)) can only be maintained for the pseudo-solution by a hypothetical positional shift in the Parameter Space, whereas the true solution acts like an anchor for each isosurface. This immediately suggests the means of a general concept to separate PSC solution volumes and identify false pseudo-solutions by using data sets of two photon energies offering different atomic scattering strength ratios, similar to resonant contrast in *Resonant X-ray Diffraction* methods. As had to be expected from symmetry considerations according to the EPA model, the pseudo-solution has a minimum standard deviation of about 1×10^{-4} for $f_{\text{La}} = f_{\text{Sr}}$ and increases by about one decade for disproportionated scattering strengths. Further, the positions of the “lighter” atoms (with smaller f) are less well-defined (see Fig. 3 (a)), which coincides with the elongation of isosurfaces in these directions (Fig. 3 (b) and Fig. 3 (c)). Although in absolute comparison La is the heavier atomic species, the errors for “light La” are higher than for “light Sr”, because Sr has the triple stoichiometric weight. In addition, the limits for the resulting lin-

ear solution vector series (red dots in Fig. 3(a)) are defined by twice the presumed difference Δz .

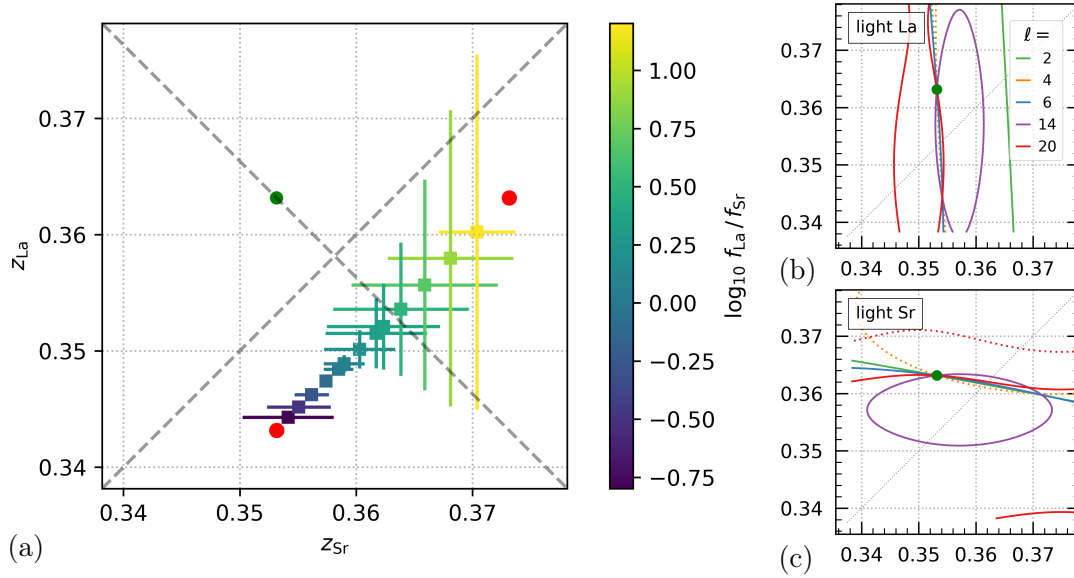


Fig. 3. (a) Model study of both the true and the pseudo-symmetric solution as a function of scattering strength ratio by fitting intersecting isosurfaces $F(l)$ (least-squares). The ratio was varied by a scaling factor of 10, keeping the mean product $f_{\text{La}} \cdot f_{\text{Sr}}$ fixed. The isosurfaces $F(l)$ were calculated for reflections $l = 2, 4, \dots, 20$. Confidence regions are given as error bars of 2.6σ , magnified by a factor of 10 for better visibility. The true solution ($z_{\text{La}}, z_{\text{Sr}}$) is independent of the varying ratio (green dot), whereas the pseudo-solutions result in a linear series between the limits at a distance $2 \cdot \Delta z$ (red dots). As expected, the positional errors scale inversely to the scattering power. The change in scattering power directly reflects the distortion of the respective isosurface features, *i. e.* light weights act as elongations that increase the respective positional errors, shown for the limits of the series in (b) for “light La” (yellow dot) and in (c) for “light Sr” (violet dot).

Step 3: Intensity Errors and Monte-Carlo Calculations

We studied the rigidity of the PSC to reveal the presumed split position with respect to reflection intensity errors by means of Monte-Carlo calculations, similar to the approach by Kirfel *et al.* [2] and later by Zschornak *et al.* [17,18], using now the DFT-predicted more realistic split of $\Delta z = 0.0034$ (≈ 4.2 pm) for three error distributions $\Delta I/I$ of 20 %, 5 % and 1 % (Fig. 4). Again, we performed the calculations with structure

factors for the full structure varying z_{La} and z_{Sr} while keeping the MnO_4 contribution fixed. To implement conditions as close as possible to experimental observations, we now analyze reflection intensities.

By applying statistically, *i. e.* Gaussian, distributed artificial intensity errors of up to 20% to the theoretical data, we obtain quite different behavior in dependence of the introduced intensity error. For the low quality data with $\Delta I/I = 20\%$, only one solution vector is allocable within the 2.6σ and 1σ confidence regions in Parameter Space. In the free z parameters of La and Sr, the statistical center of the best fits is the high symmetry position. Hence, low quality data cannot identify two separate solutions. However, they may provide a hint: and by using better measurements, this hint gets confirmed [18]. For the medium quality data with $\Delta I/I = 5\%$ two distinct solution vectors (Fig. 4) become evident within the σ confidence region, confirming a split position. Only few random error distributions result in the high symmetry solution at the central region of the depicted Parameter Space. For the high quality data with $\Delta I/I = 1\%$, the split positions are the clear structure solution, with the pseudo-symmetric solution well separated as a second solution vector.

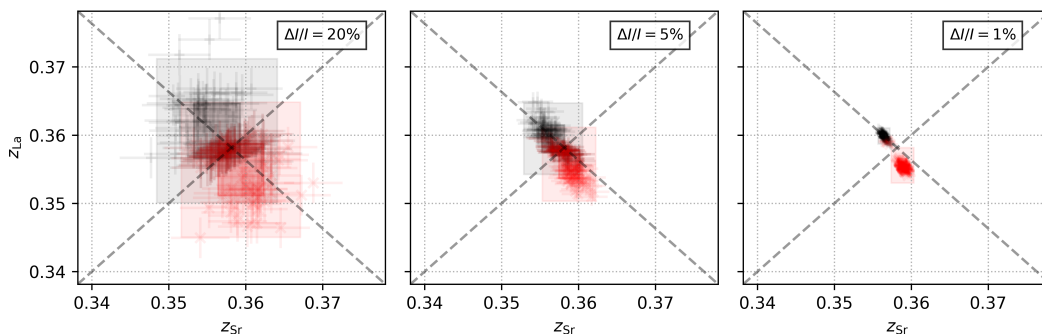


Fig. 4. Monte-Carlo study of the split position with $\Delta z = 0.01$ for different Gaussian distributed random errors on the reflection intensities for $l = 2, 4, \dots, 20$ with 100 test samples each (least-squares fits). The solution is in black, the pseudo-solution in red, each with two confidence regions $1\sigma \approx 68\%$ and $2.6\sigma \approx 99\%$.

In conclusion, the split along the z axis can be well resolved as 0.0034 ± 0.0003 , corresponding to approx. (4.2 ± 0.4) pm, for sufficiently good data quality. The positional least-square fit errors from random intensity errors are dominant in comparison to the fit errors from disproportionated scattering factors of the pseudo-solution (Step 2, magnified by a factor of 10 in Fig. 3).

Step 4: Dependence of the Resolution on the Intensity Error

We tried to answer the question: “What is the smallest difference Δz that can be separated with a confidence level of $2.6\sigma = 99\%$ by the above Monte-Carlo calculations?” Figure 5 shows Monte-Carlo simulations of the $(\text{La}_{0.5}\text{Sr}_{1.5})\text{MnO}_4$, $I4/mmm$, structure for a series of different z_{La} and z_{Sr} input values and for different assumed data qualities. The resulting fits represent overlapping error envelopes for the z_{Sr} and z_{La} position, respectively. For medium quality data with $\Delta I/I = 5\%$ a Δz of 0.007 can be separated, which corresponds to 8.5 pm. For $\Delta I/I = 1\%$, a resolution of $\Delta z > 0.003$ (3.7 pm) is possible. The precision of the method is even much ($> 10^1$) better in finding the respective solution vectors. Further, it is evident what has already been found in Step 2: for poor data quality $\Delta I/I = 20\%$ the split position cannot be verified within the calculated Δz range.

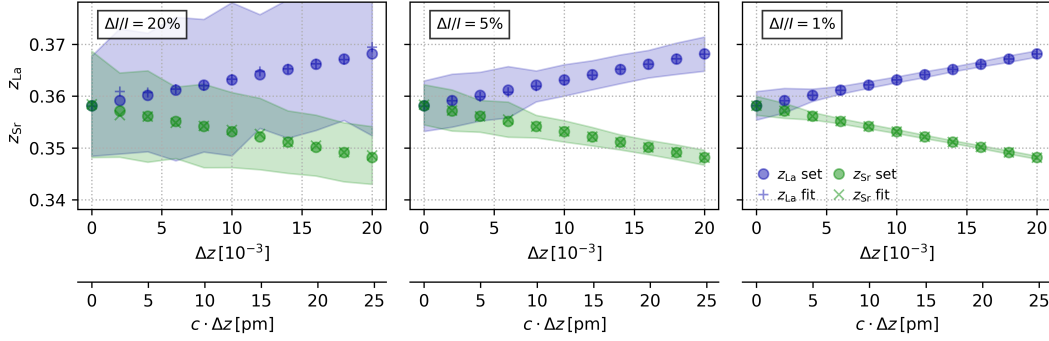


Fig. 5. Fitted positions z_{La} (blue +) and z_{Sr} (green x) for a series of presumed splits $0 \leq \Delta z \leq 0.02$ (between green and blue circles, accordingly) and three data qualities, given with a confidence level of 99 % (error envelopes, 100 samples each, least-squares fit). For the three different intensity errors $\Delta I/I = 20\%$, 5% and 1% , the distinct split positions can be resolved for splits $\Delta z > 0.02$ (≈ 25 pm), $\Delta z > 0.007$ (≈ 8.5 pm) and $\Delta z > 0.003$ (≈ 3.7 pm), respectively.

Step 5: Pushing the Limits of the PSC

Here, we offer an estimate of the maximum resolution that may be achieved based on enhanced resonant scattering contrast as well as on extraordinary data quality with $\Delta I/I = 1\%$, *e.g.* at synchrotron conditions. For this purpose, we consider two different X-ray photon energies: one far away and one just below the Sr-*K* absorption edge at 15 keV and 16.1 keV, respectively. For the lower energy, the atomic scattering factors are used as before and for the higher energy a resonant scattering correction of $f'_{Sr} \approx -7.4$ electrons is applied ($f''_{Sr} \approx 0$) [13].

Regarding the pseudo-solution, the relative influence of this constant correction to the scattering power of Sr is different for each reflection, and therefore the deformation of the according isosurface as well. The pair-wise intersections are thus distributed for the pseudo-solution in the pm range. For low indexed reflections $l \leq 10$ this effect appears like two accumulation points along the linear relation depicted in Fig. 3. (Fig. 6, inset upper right). Including higher indexed reflections, the distribution of isosurface in-

tersections becomes even broader and the volume of the pseudo-solution “blurs” (Fig. 6, inset lower right), whereas the true solution remains sharp. Consequently, as long as error margins of the isosurfaces are sufficiently small, the pseudo-solution can be identified as a “false” solution, which is incompatible with experimental observations. In classical X-ray diffraction analysis, the existence of the second solution as a case of quasi- or pseudo-symmetry will remain as long as the atomic shift is less than the optical resolution of a standard data set.

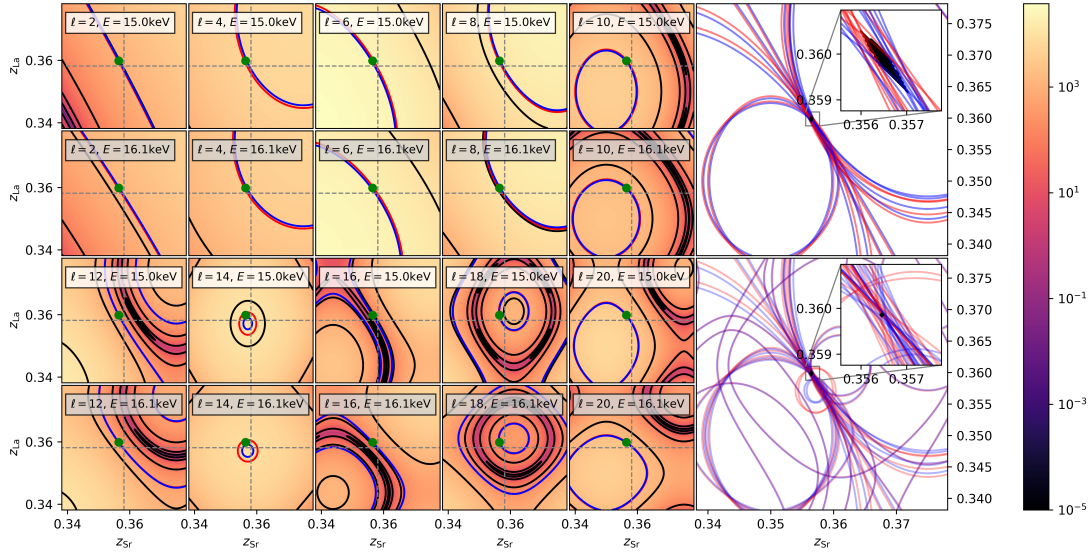


Fig. 6. 2-dimensional Parameter Space $z_{\text{Sr}} \otimes z_{\text{La}}$ for the structure $(\text{La}_{0.5}\text{Sr}_{1.5})\text{MnO}_4$, $I4/mmm$, in the vicinity of the split position (green dot). The diffraction data are given as intensity isosurfaces $I(l)$ for two photon energies $E = 15\text{ keV}$ and $E = 16.1\text{ keV}$ (just below the Sr absorption edge) and for error envelopes of $\pm 1\%$ (blue and red line). The contrast enhancement and respective superior resolution (small black region) originate from multiple large-angle intersections (upper right $l = 2, 4, \dots, 10$; lower right $l = 2, 4, \dots, 20$), and especially the small envelope of the low-intensity high-indexed reflection 0016 (increased opacity in lower inset). In addition, the second wavelength severely lifts the degeneracy of the pseudo-solution.

Further, we focus on the sharp solution, which is equivalent to studying the sheer difference Δz , without the discussion of the pseudo-solution. Specifically, Fig. 6 demonstrates that reflections with low indices show a strong covariance for an antisymmet-

ric change in positions; and especially the reflection 0014 lifts this correlation. We achieved an estimated theoretical precision in the z coordinates of ± 0.00015 corresponding to about ± 0.19 pm (Fig. 6). This seemingly extreme value is due to strong gradients of high indexed reflections [18], here valid especially for both energies of reflection 0016. Additional improvements are in principle possible, *e.g.* if high indexed small amplitudes are available presenting strong relative resonant contrast.

4. Discussion

The present work is a feasibility study based on synthetic data. It is, however, close to reality because several typical intensity error distributions have been considered in the framework of kinematic diffraction. While abandoning the EPA model (Step 1, generally better for neutron diffraction), we prove both, the enhanced resolution and precision of the coordinates by f' contrast (Steps 2 and 5). Compared with preceding work [17, 18], further qualitative and quantitative progress is achieved, as we now resolve realistic splits in the order of 4 pm (Step 3 and 4), as indicated by our preliminary DFT modeling.

In terms of resolution limits, the PSC offers a very high theoretical precision, even well below the 1 pm range, when additionally using resonant contrast enhancement for the discussed 2-dimensional Parameter Space case. The result is feasible, since the method does not rely on Fourier inversion and the positional uncertainty is therefore not determined by the conventional diffraction limit representing an incomplete plane wave basis set, but rather directly by the absolute intensity (normalized on the primary beam) errors. The resolution of ± 0.19 pm is comparable with that of Richter *et al.* [16]. Instead of fitting full spectra, here we employ precise standard reflection amplitudes for two wavelengths. Nevertheless, as soon as intensity errors are considered within a typical range between 5 % and 20 %, the precision drops significantly, here to about

10 pm, and pseudo-symmetries based on static atomic displacements smaller than that limit cannot be resolved. The influence of real structure and temperature effects on the resolution is in the focus of ongoing research and will be discussed in consecutive work. In principle, isotropic as well as anisotropic atomic displacement parameters may be treated within the PSC methodology as additional degrees of freedom.

In particular, the qualitative changes of isosurfaces due to resonant scattering contrast, *i. e.* their individual elongations and contractions, offer unique dependencies to further restrict the solution volume in Parameter Space. As demonstrated here for the La/Sr split position in the structure of $(\text{La}_{0.5}\text{Sr}_{1.5})\text{MnO}_4$, this contrast may even help to reveal pseudo-symmetric solutions, as they move in Parameter Space with variation of the atomic scattering power ratios, while the “true” solution will remain fixed (Step 2). In general, model calculations of isosurfaces (preferably close to the solution region) can provide hints for precise measurement of selected reflections that, in turn, lead to highly precise structure solutions (see text after Fig. 2). The influence of f'' , considering supplementary absorption effects, must still be investigated. Work on how a relevant f'' , apart from being 0 or π , acts on the reflection phases is in progress.

The presumed shift $\Delta z \approx 0.0034$ (4.2 pm) is obtained twice in the PSC picture: (i) precisely by the coordinate difference of the sharp solution (*e. g.* Fig. 6) and (ii) less well defined by the separation between both solutions (confidence regions in Fig. 4 and Fig. 5). A further “free” z parameter exists in the structure: that of O2 [8], also occupying a 4e Wyckoff site, exactly as Sr/La. Due to the split of La/Sr, this adjacent oxygen is affected as well, which might give rise to a second z split for this 4e position. In a 4-dimensional Parameter Space, the oxygen displacement may also be determined by PSC together with those of Sr and La, based on 00 l data.

5. Conclusion and Outlook

In summary, the article revises the application of the recently developed PSC method to resolve the La/Sr split position within the reported crystal structure of the potential high-temperature super-conductor $(\text{La}_{0.5}\text{Sr}_{1.5})\text{MnO}_4$. Based on methodical enhancements abandoning the Equal Point Atom Model and varying the La/Sr scattering contributions by means of resonant contrast the formerly found systematic offset in the determined solution vector could be eliminated. The originally proposed pseudo-solution could be identified as incompatible with theoretical amplitudes of $00l$ reflections ($l = 2, 4, \dots, 20$). Further, the postulated shift in the order of 4 pm could be well-revealed for sufficiently good data quality.

To our best knowledge, resolution limits within the PSC have no theoretical basis yet, as compared to the complete “theoretical optics” for the “optical picture” of scattering densities. The consequences of intensity errors broadening the isosurface restrictions, and respectively the solution region, strongly depend on the specific structure. In general, the arising dependencies show non-linear behavior and result in an inverse problem. $(\text{La}_{0.5}\text{Sr}_{1.5})\text{MnO}_4$ did not offer small and uncorrelated $00l$ amplitudes at the same time. Thus, the optimal resolution of the PSC methods was not reached.

In terms of resolution limits, the PSC offers a very high theoretical precision, even well below the 1 pm range when additionally using resonant contrast enhancement. Similar resolution as for the here discussed 2-dimensional Parameter Space case can be expected for any structural problem. The result is feasible, since the method does not rely on Fourier inversion and the error is therefore not determined by the conventional diffraction limit, but by the absolute intensity errors. We plan to further work on that and hope this study adds to reveal these limits.

By reducing the Parameter Space (of a given substance) to a subspace covering only the equipoints in question, the high-dimensional data set is correspondingly reduced

to much less reflection amplitudes necessary for solving this specific problem, as was shown here for the La/Sr split position. Since only few reflections or amplitudes are sufficient (and not a complete XRD data set), this approach is especially interesting for studying time-dependent processes in already known crystal structures, e.g. during phase transformations, dynamic transport processes, etc. In most cases, these reflections can be precisely specified in a preliminary analysis. This makes the PSC very attractive for *in-situ* diffraction at synchrotron beamlines to localize or detect smallest changes of atomic positions in material systems with known atomistic models, which meets current demands of *in-situ* and *in-operando* research.

Acknowledgements: The authors acknowledge funding by the DFG within the project DFG 442646446, ZS 120/5-1. Additional funding was provided within DFG 409743569, ZS 120/1-1 as well as through public funds from the Federal Ministry of Education and Research and the State of Saxony SN0390002. Part of the work was conducted within the CREMLINplus project, which received funding from the European Union's Horizon 2020 research and innovation programme under grant agreement No. 871072. The authors cordially thank Dmitri V. Novikov (DESY) for his intense reading of the manuscript and appreciated comments, Muthu Vallinayagam for his help with the preliminary DFT calculations, as well as Prof. Dirk C. Meyer for providing ideal research conditions at the ZeHS. MZ, CW, and KF would like to extend a special thank you to Melanie Nentwich as she continues to be very close to her former colleagues through her valuable support of ongoing projects.

References

- [1] K. F. Fischer, A. Kirfel, and H. W. Zimmermann. Structure determination without Fourier inversion. Part I. Unique results for centrosymmetric examples. *Z. Kristallogr.*, 220:643, 2005. <https://doi.org/10.1524/zkri.220.7.643.67099>.
- [2] A. Kirfel and K. F. Fischer. High Resolution Structure Determination without Fourier Inversion: Study of a one-dimensional Split Position. Poster at the Annual Conference of the German society for Crystallography, March 2005.

- [3] K. F. Fischer, A. Kirfel, and H. W. Zimmermann. A Concept for Crystal Structure Determination without FOURIER Inversion Part III. Some Steps towards Application. *Croat. Chem. Acta.*, 81:381, 2008. <https://hrcak.srce.hr/file/44706>.
- [4] A. Kirfel and K. F. Fischer. Structure determination without Fourier inversion. Part IV: Using quasi-normalized data. *Z. Kristallogr.*, 224:325, 2009. <https://doi.org/10.1524/zkri.2009.1130>.
- [5] H. W. Zimmermann and K. F. Fischer. Structure determination without Fourier inversion. Part V. A Concept based on parameter space. *Acta Crystallogr.*, A65:443, 2009. <https://doi.org/10.1107/S0108767309030293>.
- [6] A. Kirfel and K. F. Fischer. Structure determination without Fourier inversion. Part VI: High resolution direct space structure information from one-dimensional data obtained with two wavelengths. *Z. Kristallogr.*, 225:261, 2010. <https://doi.org/10.1524/zkri.2010.1241>.
- [7] K. Pilz. *Weiterentwicklung und Anwendung einer algebraischen Methode zur Teilstrukturbestimmung, ein Beitrag zur Eindeutigkeit von Strukturanalysen*. PhD thesis, Universität des Saarlandes, Saarbrücken, 1996.
- [8] D. Senff, P. Reutler, M. Braden, O. Friedt, D. Bruns, A. Cousson, F. Bourée, M. Merz, B. Büchner, and A. Revcolevschi. Crystal and magnetic structure of $\text{La}_{1-x}\text{Sr}_{1+x}\text{MnO}_4$: Role of the orbital degree of freedom. *Phys. Rev. B*, 71:024425, Jan 2005.
- [9] S. Lippmann, T. Kiele, J. Geck, P. Reutler, M. von Zimmermann, and B. Büchner. Charge density study of $\text{La}_{0.5}\text{Sr}_{1.5}\text{MnO}_4$ at room temperature. DESY Annual Report, 2003. http://hasyweb.desy.de/science/annual_reports/2003_report/part1/contrib/42/9852.pdf.
- [10] G. Kresse and J. Furthmüller. Efficiency of ab-initio total energy calculations for metals and semiconductors using a plane-wave basis set. *Computational materials science*, 6(1):15, 1996.
- [11] A. Kirfel and K. F. Fischer. High Resolution Structure Determination without Fourier Inversion: Study of a one-dimensional Split Position. *Z. Kristallogr. Suppl.*, 21:101, 2004. Abstract to [2].
- [12] J. Karle. Some anomalous dispersion developments for the structure investigation of macromolecular systems in biology. *Int. J. Quantum Chem. Symp.*, 7:357, 1980.
- [13] S. Sasaki. KEK Report 90-16. *National Laboratory for High Energy Physics, Tsukuba*, page 7, 1990. <http://www.sasakiken.net/reports/reports.html>.
- [14] Y. Joly, S. D. Matteo, and O. Bunău. Resonant X-ray diffraction: Basic theoretical principles. *Eur. Phys. J. Spec. Top.*, 208:21, 2012. <https://doi.org/10.1140/epjst/e2012-01604-5>.
- [15] M. Zschornak, C. Richter, M. Nentwich, H. Stöcker, S. Gemming, and D. C. Meyer. Probing a crystal's short-range structure and local orbitals by Resonant X-ray Diffraction methods. *Cryst. Res. Technol.*, 49:43, 2014. <https://doi.org/10.1002/crat.201300430>.
- [16] C. Richter, M. Zschornak, D. Novikov, E. Mehner, M. Nentwich, J. Hanzig, S. Gorfman, and D. C. Meyer. Picometer polar atomic displacements in strontium titanate determined by resonant X-ray diffraction. *Nat. Commun.*, 9:178, 2018. <https://doi.org/10.1038/s41467-017-02599-6>.

- [17] M. Zschornak, M. Nentwich, D. C. Meyer, A. Kirfel, and K. F. Fischer. Advances in the Parameter Space Concept for Crystal Structure Determination – use of neutron diffraction data and resolution study. *Z. Kristallogr. Suppl.*, 40:59, 2020. <https://doi.org/10.1515/9783110692914-002>.
- [18] M. Zschornak, C. Wagner, M. Nentwich, D. C. Meyer, and K. F. Fischer. Advances in the Parameter Space Concept for Crystal Structure Determination – A maximum Resolution Study. *Acta Crystallogr.*, A77:C1254, 2021.

Synopsis

The *Parameter Space Concept* (PSC) is an alternative approach to determine crystal structures from diffraction intensities of standard Bragg reflections without the use of Fourier transforms. Here, we present a resolution study of the PSC for an example of a La/Sr split position in the potential high-temperature super-conductor $(\text{La}_{0.5}\text{Sr}_{1.5})\text{MnO}_4$ with sub-picometer resolution beyond $\lambda/\sin\theta_{\max}$ from (rather) few reflections.
